MLM-2884

Mound Facility Activities in Chemical and Physical Research: January-June 1981

December 15, 1981

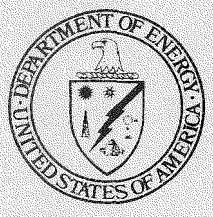

Monsanto

MOUND FACILITY
Miamisburg, Ohio 45342

operated by
MONSANTO RESEARCH CORPORATION
a subsidiary of Monsanto Company

for the
U. S. DEPARTMENT OF ENERGY
Contract No. DE-AC04-76-DP00053

Printed in the United States of America
Available from
National Technical Information Service
U. S. Department of Commerce
5285 Port Royal Road
Springfield, VA 22161

NTIS price codes
Printed copy: A03
Microfiche copy: A01

MLM--2884

DE82 006218

Mound Facility Activities in Chemical and Physical Research: January-June 1981

Issued: December 15, 1981

MOUND FACILITY
Miamisburg, Ohio 45342

operated by
MONSANTO RESEARCH CORPORATION
a subsidiary of Monsanto Company

for the
U. S. DEPARTMENT OF ENERGY

Contract No. DE-AC04-76-DP00053

Foreword

This report is issued semiannually by Mound Facility. Under the sponsorship of the DOE Division of Basic Energy Sciences, Mound Facility is responsible for research in the physical sciences to further the progress of science and technology in the public interest. This report is submitted by W. T. Cave, Director of Nuclear Operations, and R. E. Vallee, Manager of Technology Applications and Development, from contributions prepared by W. M. Rutherford, Science Fellow (Thermal Diffusion); W. L. Taylor, Science Fellow (Gas Dynamics and Cryogenics); G. L. Silver, Science Fellow (Separation Chemistry); L. J. Wittenberg, Leader, Metal Hydride Research; and from members of the Isotope Separation Section: W. R. Wilkes, Isotope Separation Manager; E. D. Michaels, Leader, Isotope Separation Engineering; and B. E. Jepson, Senior Research Specialist, Metal Isotope Separation Research and Development.

These reports are not intended to constitute publication in any sense of the word. Final results either will be submitted for publication in regular professional journals or will be published in the form of MLM topical reports.

Previous reports in this series are:

MLM-2168	MLM-2506
MLM-2198	MLM-2555
MLM-2241	MLM-2590
MLM-2296	MLM-2654
MLM-2354	MLM-2727
MLM-2414	MLM-2756
MLM-2450	MLM-2809

Contents

I. Low temperature research

II. Separation research

III. Metal hydride studies

I. Low temperature research

Reaction rates of deuterium-tritium mixtures

G. T. McConville, D. A. Menke, and R. E. Ellefson

Experiments measuring the rate of reaction of D_2 and T_2 mixtures in the mixing chamber described in MLM-2756 [1] are in progress. The first experiments at room temperature have produced some interesting results. In order to understand the results, the mixing chamber must be described in some detail, and a diagram of it is shown in Figure I-1. The 2 liter containers for the pure components are connected to the mixing chamber by 40-mil i.d. capillary lines. The lines terminate in the center of the mixing chamber. A 10-mil i.d. capillary 6 ft long directs samples to the mass spectrometer sampling system.

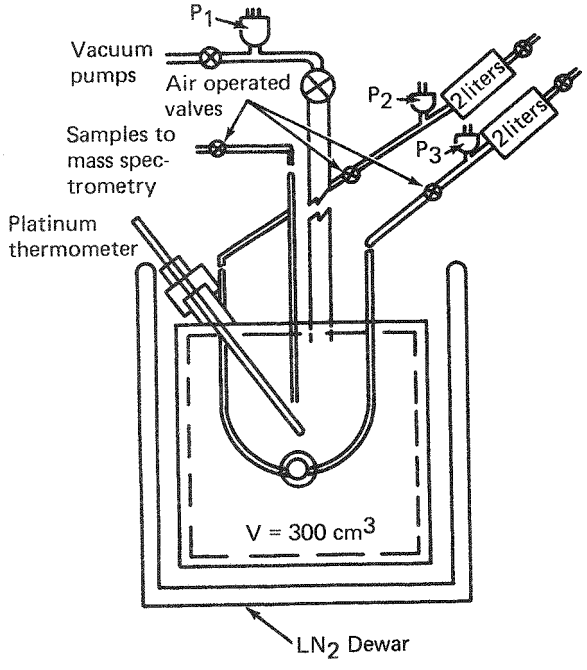

FIGURE I-1 - Schematic representation of mixing chamber for D_2+T_2 reaction rate experiments.

Once the sample enters the sampling system, the sample pressure is reduced to less than 1 torr which halts further equilibration of the sample. The sampling process takes from 2 to 3 cm^3 of material from the mixing chamber.

The initial experiments were done with 300 mm of a 30% T_2, 70% D_2 mixture. The reaction rate k can be obtained from the following equations:

$$\ell n\left[1 - \frac{DT(t)}{DT(\infty)}\right] = kt \quad \text{or} \quad \ell nQ = kt$$

$$\ell n\left[\frac{D_2(o)-D_2(t)}{D_2(o)-D_2(\infty)}\right] = kt \qquad (1)$$

$$\ell n\left[\frac{T_2(o)-T_2(t)}{T_2(o)-T_2(\infty)}\right] = kt$$

An example of the data in this form is shown in Figure I-2. The reaction can be seen to be first order over about 98% of the reaction. There is a slight difference in k for the three components. These results can be compared to the only other results for DT, those of Pyper, et al. [2] shown in Figure I-3, which show widely different values of k for the different components. The present results appear to be more consistent. We found that trying to mix the components simultaneously produced backstreaming into the low pressure, pure component 2-liter container. Therefore, the T_2 was put in first, and D_2 followed within 10 min.

We intended to do five experiments with a 30/70 T_2-D_2 mixture at 300 mm pressure to test the reproducibility of the mixing chamber. On the third experiment, however, the computer malfunctioned on the mass

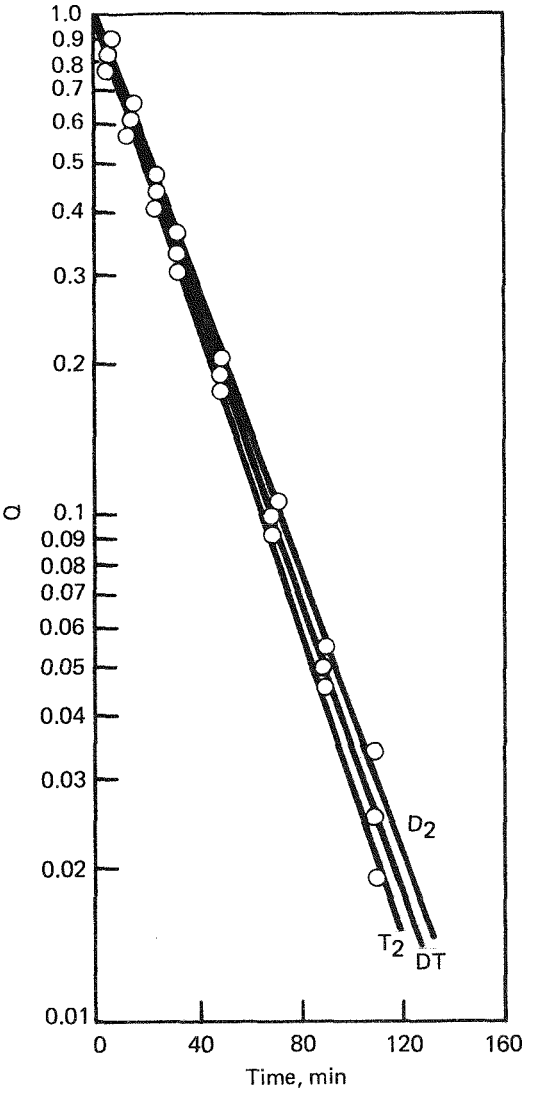

FIGURE I-2 - Reaction plot for D_2, T_2, and DT components, Q represents the arguments of the logarithms for the three cases in Equation 1.

spectrometer after the T_2 was put into the chamber, delaying the addition of D_2 to the mixture by 24 hr. In this experiment the reaction went three times slower. This serendipitous result led to a series of experiments, the results of which are shown in Table I-1 and Figures I-4 and I-5. What appears to be clear from the first eight experiments in Table I-1 is that the speed of the reaction depends on which gas has been in the container first, and that the conditions (e.g., runs 3 and 6 or 1, 2, and 8) can be reproduced. Runs 4 and 5 indicate that there may be a memory of the conditions of run 3, but soaking with D_2 (run 7) wipes out the effect between runs 6 and 8. In Figure I-4 the DT(t) results are shown for experiments 6, 7, 8, with a total pressure of 300 torr. In Figure I-5 the results of experiments 9, 10, 11, are shown for a pressure of 150 torr and the same respective conditions of runs 6, 7, 8. Comparing runs 3, 6, and 10 shows no pressure dependence of the reaction when T_2 is allowed to stand in the mixing chamber for 24 hr before mixing, whereas a small pressure dependence is seen in comparing runs 7 and 11 or 8 and 9. Run 12 is an extension of the conditions of runs 8 and 9 to 500 torr. There appears to be no increase in reaction rate when the two components are mixed at the same time above 300 torr. Runs 13 and 14 show the effect of varying the T_2 concentration in the mixture. The rate of reaction increases with T_2 concentrations as one might expect.

The results, other than runs 13 and 14, are difficult to fit to a consistent explanation. At the moment we have two hypotheses. One is that a catalytic reaction on the surface of the container is the rate controlling reaction. The container is of specially processed 304 stainless steel constructed by Quantum Mechanics, Inc., Tracy, Ca. The surface is etched and then vacuum baked at 600°C. This process produces a nearly iron free (a few ppm) surface and a surface area about two or three times the ideal area according to their SEM studies. How much oxide is on the surface is open to question. Prior to this set of measurements, the container was soaked with T_2 (less than 1% ^3He) for several days. The

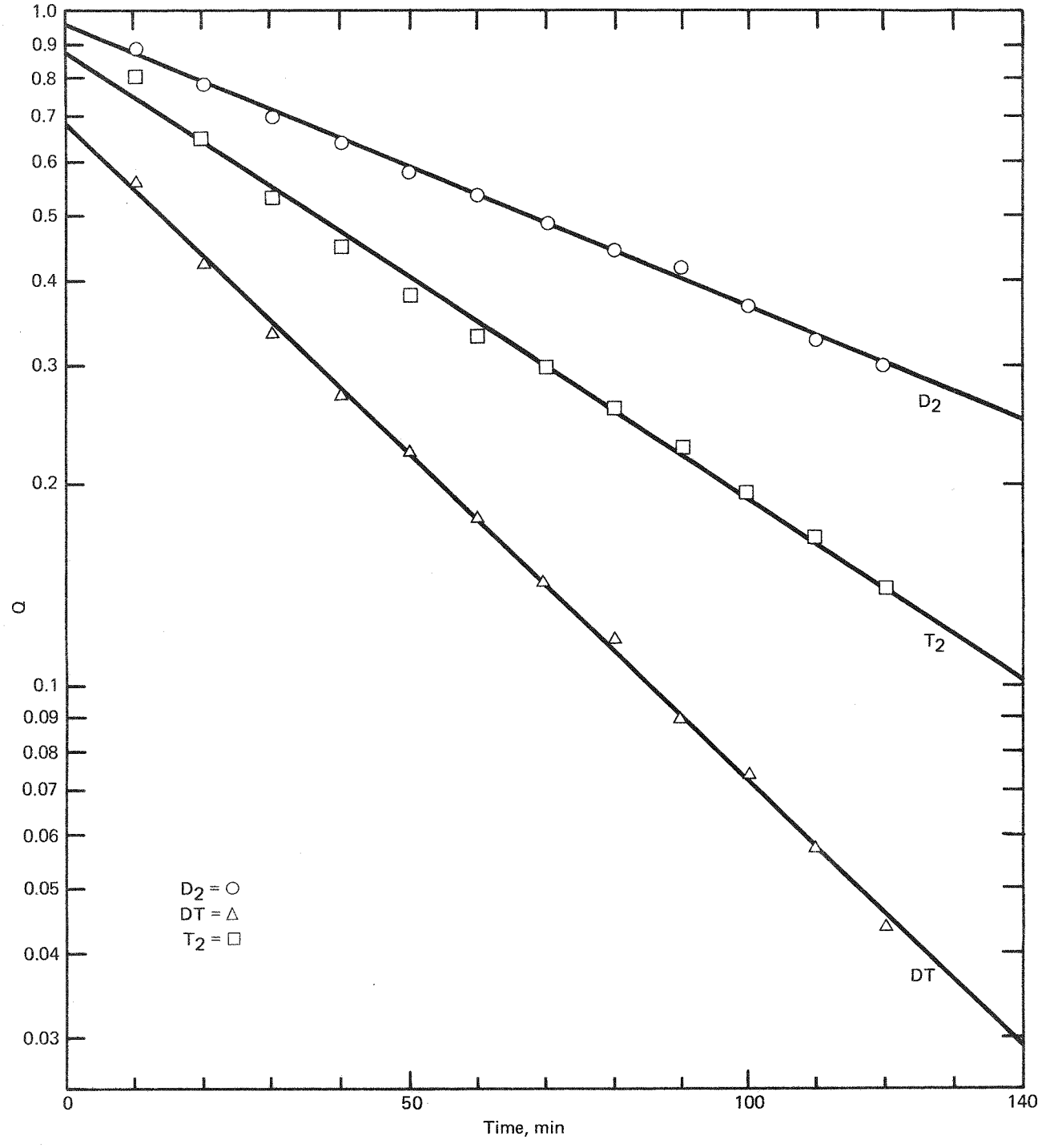

FIGURE I-3 - Reaction rates from Reference 2 for similar temperature and T_2 concentration.

Table I-1 - REACTION TIMES FOR D_2 + T_2 EXPERIMENTS

Experiment	Pressure (torr)	t_1 (min)	Condition
1	300	32	30% T_2 mixed together
2	300	36	30% T_2 mixed together
3	300	86	30% T_2 in 24 hours
4	300	52	30% T_2 mixed together
5	300	42	30% T_2 mixed together
6	300	84	30% T_2 in 24 hours
7	300	29	30% D_2 in 24 hours
8	300	34	30% T_2 mixed together
9	150	47	30% T_2 mixed together
10	150	84	30% T_2 in 24 hours
11	150	39	30% D_2 in 24 hours
12	500	34	30% T_2 mixed together
13	455	16	55% T_2 mixed together
14	300	94	10% T_2 mixed together

protium content in the form of HT in the T_2 after the last soak was approximately 0.05%. The T_2 in the Quantum Mechanics 2-liter storage container we are using shows HT <0.01%. Now, when one exposes a nickel-chromium or nickel-chromium oxide surface to hydrogen isotopes, a chemisorbed layer of atoms is formed which can easily exchange with the gas [3]. When the reaction starts, about 1 or 2 parts in 10^4 of the hydrogen isotopes in the container are in the chemisorbed layer. As the reaction proceeds, the composition of the layer and therefore the rate of reaction should change. However, this is not what is seen. The reaction appears to be simple first order in time in all the experiments for about 95 to 98% of completion.

The second hypothesis is that the reaction is indeed a chain reaction in the gas, and the presence of T_2 in the container before the mixing is forming T_2O or CT_4 from the wall to the order of 1 part in 10^3, which is acting as an inhibitor for the reaction [4]. Many inhibitors are known for the T_2+D_2 reaction which can reduce the reaction rates by about a factor of 3 when present in the above quantity. T_2O at that level would be hard to detect in the capillary system. If the reaction is in the gas phase, the zero order pressure effects are hard to understand.

Experiments are under way that vary the length of time the T_2 is in the container before mixing. Also, a vacuum bake of the container at 300°C should drive off any adsorbed T_2O. These experiments may confirm one or the other of the above hypotheses. A glass mixing chamber has been designed for continuing experiments. In the glass container the hydrogen adsorption should be in molecular rather than atomic form.

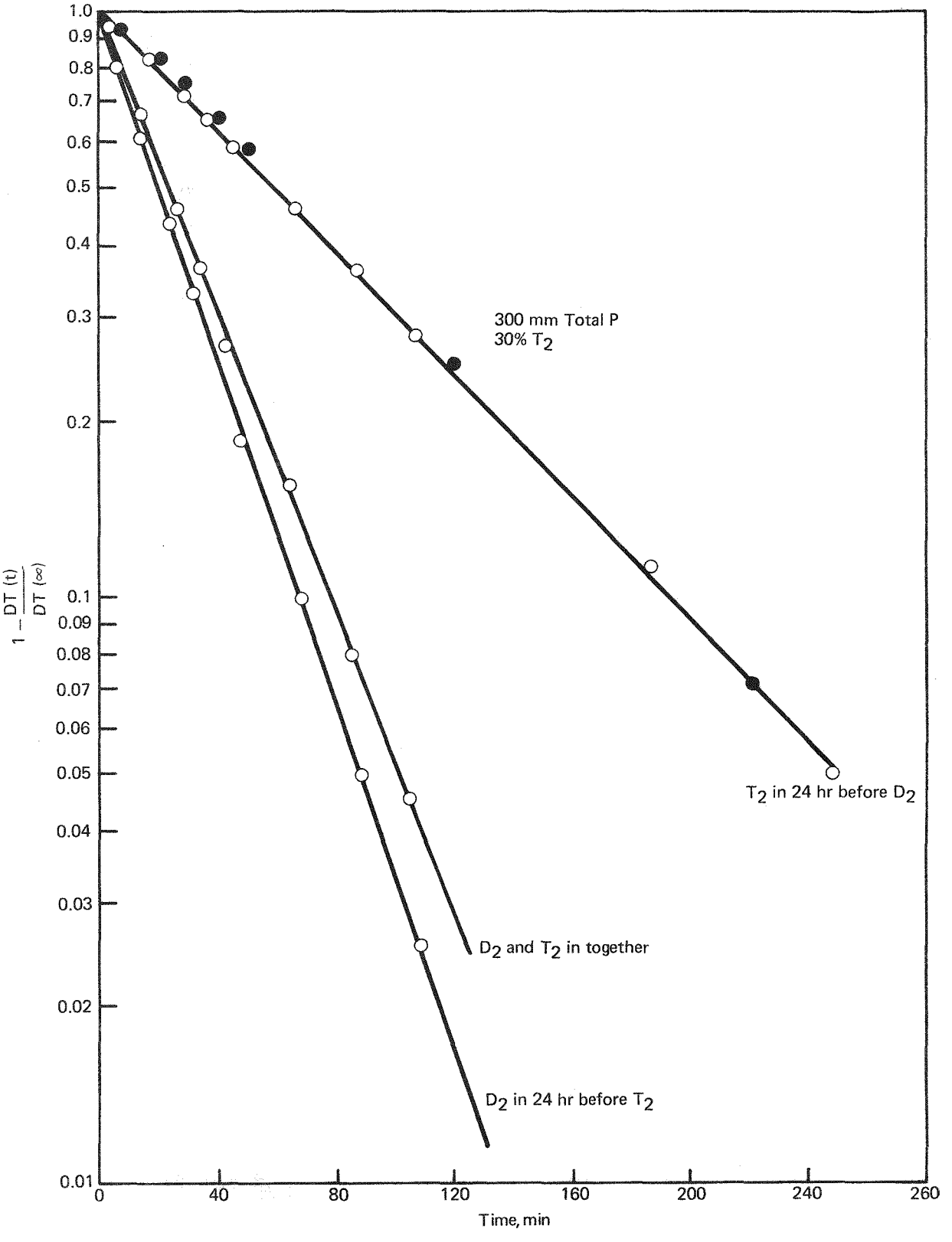

FIGURE I-4 - Reaction plot for runs 6, 7, and 8 for 30% T_2 and total pressure 300 torr. The ● represents run 3 (see text).

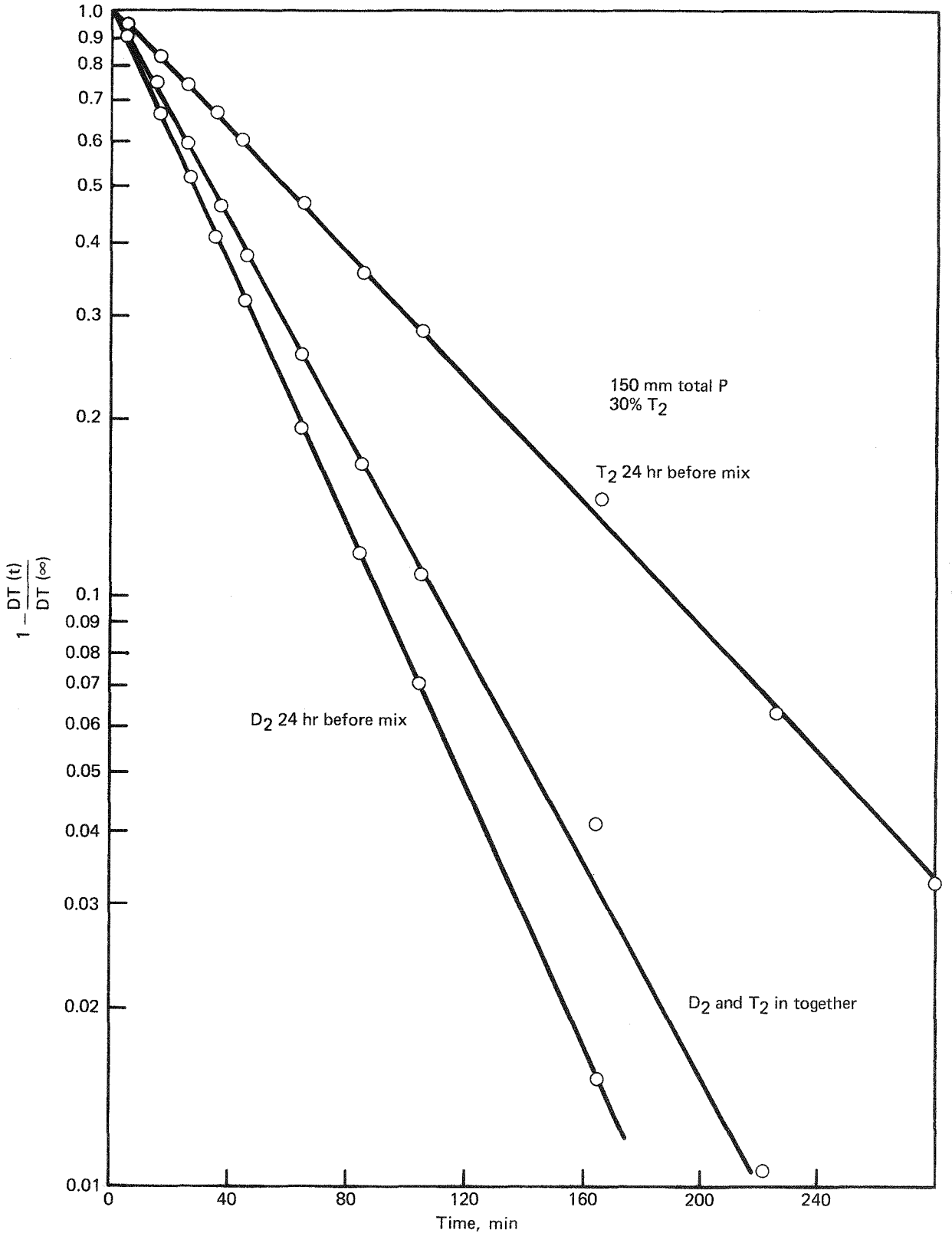

FIGURE I-5 - Reaction plot for runs 9, 10, and 11 with conditions same as in Figure 4, except total pressure is 150 torr.

Low temperature trennschaukel

D. Cain and W. L. Taylor

A twelve-tube, low temperature trennschaukel has been modified in order to study the temperature dependence of the thermal diffusion factor of binary gas mixtures from approximately 250 K to about 25 K. Two of the tubes from the apparatus were sacrificed, leaving ten tubes connected in series for the swing separation. One of the deleted tubes has been converted to a small two-bulb apparatus; the other will be used for reference cells in an in situ thermal conductivity gas analysis system. Appropriate adapters were machined to facilitate these alterations.

The twelve-tube device was similar in design to a seven-tube trennschaukel used previously at Mound [5]. Twenty-four cylindrical copper caps were machined to a depth of 5.08 cm and 1.854 cm i.d. The open end of one of these caps was silver soldered onto opposite ends of twelve thin-wall stainless steel tubes, each 10.00 cm long and 1.854 cm i.d. Each cap contained a heat exchanger of copper wool held in place by a copper screen. The bottom of each of the first eleven tubes was connected to the top of the next tube by a 23 cm length of 0.108 cm i.d. thin-wall stainless steel tubing. The top of the first tube and the bottom of the twelfth were to be connected to opposite ends of a bellows pump in order to swing a quantity of gas to and fro. The axes of the tubes were equally spaced on a 4 in. diam circle, and opposite ends were silver soldered to 1/4 in. thick by 5 in. o.d. copper disks to ensure good thermal contact.

Figure I-6 shows a schematic diagram of the modified trennschaukel/two-bulb apparatus (TS/TB) with the reference cells for the thermal conductivity gas analysis. The schematic shows the tubes connected to the copper plates in a linear fashion. The stainless steel center sections of the sacrificed tubes were machined off in a mill at the copper-stainless steel joint. Brass caps were fabricated for the copper stubs left behind after the milling and were soft-soldered in place. For the two-bulb apparatus (TB), the brass caps had 1/8 in. holes cut in their centers for a thin-walled, stainless steel connecting tube. This tube is 0.267 cm i.d. and 9.81 cm in overall length with 9.30 cm exposed length. For the reference cells, the brass caps had 5/8 in. holes cut in their centers for the mounting of electrical feed-throughs. In addition, brass fittings were machined and mounted over holes cut into the walls of the copper portions of several of the tubes. These are indicated by the circles shown on the following tubes in Figure I-6: top of tube #1, bottom of tube #5, bottom of tube #10, top of TB and bottom of TB.

Cryogenic thermistors will be mounted onto electrical feed-throughs, and these will be soft-soldered onto the brass fittings. Two such thermistor/feed-through assemblies will be soldered to the brass fittings on the ends of the reference cells, closing off the open end of those copper tubes. Another assembly will be soldered to the brass fittings mounted on the walls at opposite ends of the TB. The fittings at opposite ends of the TS (i.e., top of tube #1, bottom of tube #10) will each hold another assembly, and a final one will be located at the bottom of tube #5. The copper wool was removed from these tubes to prevent their interfering with the thermistors.

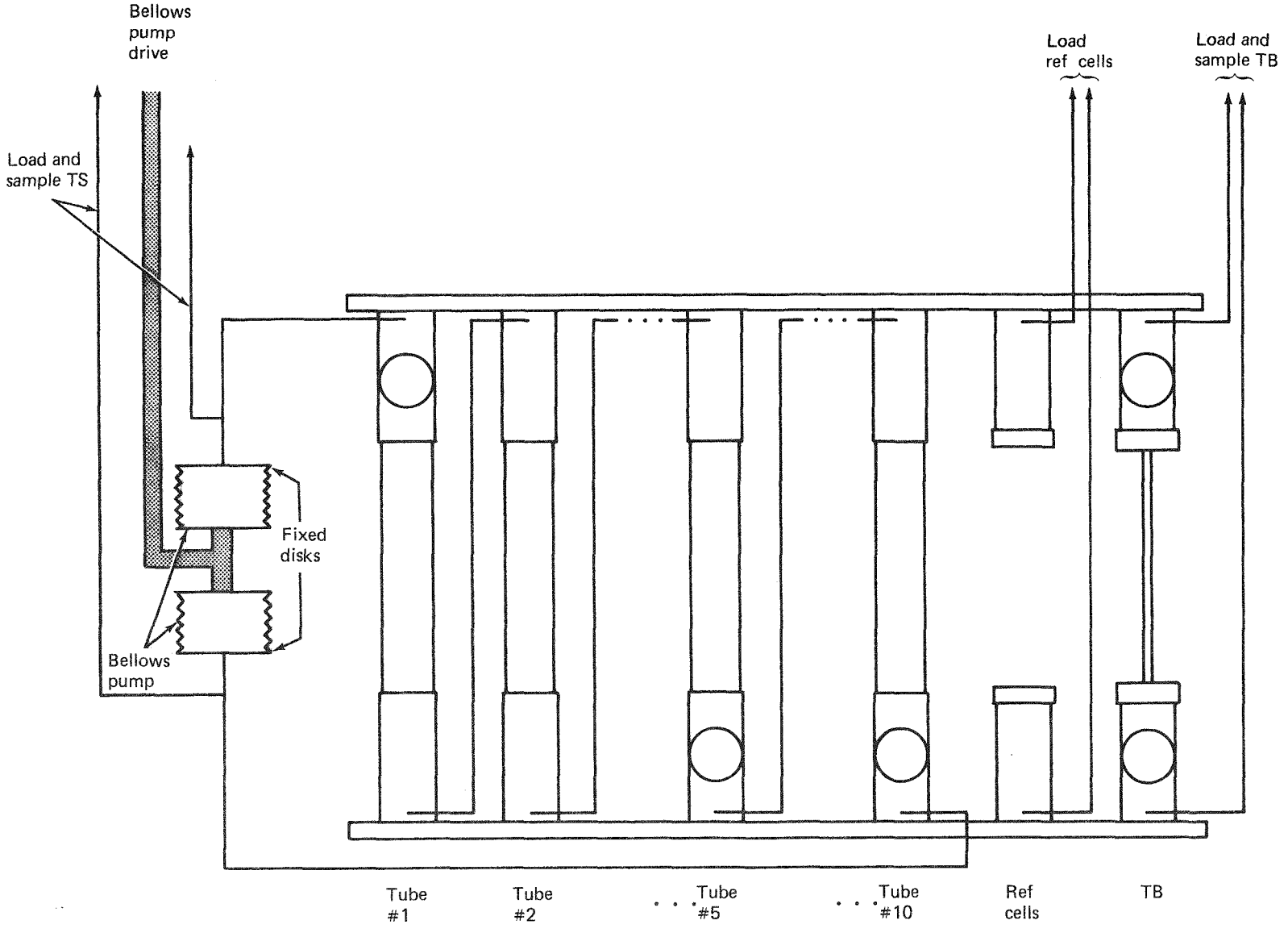

FIGURE I-6 - Schematic diagram of the modified trennschaukel/two-bulb (TS/TB) apparatus with reference cells. The tubes are shown connected to the copper plates in a linear fashion for ease of visualization. The center sections of the TS/TB and the connecting tubes are thin-wall stainless steel, the fittings (caps on TB and reference cells, thermistor mounts indicated by circles) are brass, and the ends of the tubes and the plates are copper. Tube identification numbers are given below the schematic of the device.

The presence of the thermistors in the apparatus will allow several determinations to be made. One of the uses of the thermistors has already been mentioned - that of a thermal conductivity gas analysis system. As detailed in previous reports [6,7], thermistors exposed to binary gas mixtures while connected in a wheatstone bridge configuration are sensitive to the composition of the mixture and can be calibrated to measure the composition with considerable precision. Since thermistors are also quite sensitive to temperature, provisions must be made for separate bridge configurations at the hot (top part of the TS/TB apparatus) and cold (bottom) ends of the device. This is the reason for the two separate reference cells in the TS/TB. Thermistors mounted in the top reference cell and in the top of tube #1 will be used to measure composition changes occurring in tube #1 during a thermal diffusion experiment in the ten-tube TS; those in the bottom reference cell and in the bottom of tube #10 will monitor composition changes in tube #10. Similarly, thermistors in the top reference cell and the top of the TB and those in the bottom reference cell and the bottom of the TB will follow composition changes occurring in a TB thermal diffusion experiment.

Corrections for trennschaukel operation were detailed in a previous report [8], where theoretical expressions were given for each correction term. These corrections are due to (1) approach to the steady state, (2) back diffusion in the capillaries, and (3) disturbance resulting from pumping. In addition to absolute, in situ composition determinations, the use of the thermistors will allow direct verification of the expressions for two of the correction terms.

The steady state in a thermal diffusion experiment is attained when the maximum separation of components of the mixture is reached and is indicated by zero flux; e.g., a time-independent concentration is established in the device. Since the in situ thermal conductivity bridge monitors profile composition changes continuously, the steady state will be unambiguously indicated by the absence of any further changes in composition at opposite ends of the apparatus. The half-life of the experiment is experimentally determined by looking back at the experimental data and finding the time at which the separation of components was at $\frac{1}{e}$ of its maximum value.

By swinging the bellows pump back and forth in a sinusoidal motion, a quantity of gas is moved through the system which, in the first and last tubes, has the amplitude and period of the bellows. In the inner tubes, however, the amplitudes of the quantities of gas being moved are smaller than those in the first and last tubes, and a phase shift relative to the bellows develops. If one pumps too slowly, backward diffusion in the capillaries destroys the gradients set up by thermal diffusion; if the pumping is too rapid, the inner tubes will be so far out of phase with the bellows that no transport takes place. Finally, if there are too many tubes in the device, the decreased amplitude of pumping in the inner tubes will also impede the transport of gas in the device (this last effect has already been considered in the design of the apparatus). The positioning of the thermistors in the bottom of tube #5 will allow the direct determination of the phase angle between that tube and the first (and tenth).

The use of cryogenic thermistors for composition analysis and for checking theoretical expressions for corrections may be limited by the ability to control temperature gradients in the apparatus. It has already been mentioned that thermistors and the output of a thermal conductivity gas analysis bridge employing thermistors are quite sensitive to pressure, absolute temperature, and fluctuations about a given temperature [6,7]. For these reasons, the hot and cold bridges must be calibrated with gas mixtures of known composition for each mixture to be studied and at the temperatures and pressures at which the experiments are to be performed. For the sake of convenience, this will limit the number of different temperatures in a given temperature range at which experiments will be performed. Unlike the room temperature thermal conductivity gas analysis system which has millikelvin temperature control, the TS/TB system can only hold a given temperature to 0.1 to 1.0 K [9]. If temperature excursions of this magnitude result in uncertainties in the mixture composition that are greater than the uncertainty of the room temperature device, then thermal diffusion factors will best be determined by withdrawing samples at the end of the experiment and analyzing them at room temperature. This can also be done as an independent check of the results if the in situ device is sufficiently precise. The attainment of the steady state will be determined only to within the uncertainty of the low temperature analysis system, and half-lives can be estimated only for the systems with larger separations. The phase shift of the pumping between the first (or tenth) and fifth tubes can be unambiguously monitored since this depends on the motion of the gas and not the composition of the gas.

The TS/TB is currently undergoing preliminary leak testing of the solder joints that resulted from the alterations. This is being done with rubber stoppers in place of the electrical feed-throughs. When testing is completed, the thermistors will be soldered in place and these joints tested for leaks. The device will then be wired and installed in the cryostat. Calibration and assessment of the analytical capabilities of the apparatus cannot begin until the device is in place in the cryostat.

II. Separation research

Liquid phase thermal diffusion

W. M. Rutherford

Experimental work on the separation of isotopic mixtures by liquid phase thermal diffusion is continuing on the following topics: 1) measurement of thermal diffusion factors in a precisely constructed research column; 2) study of column performance and the development of designs and techniques to eliminate or minimize nonideal behavior associated with parasitic remixing; and 3) development and operation of small separation cascades for the experimental evaluation of techniques for separating practical quantities of stable isotopes.

ISOTOPIC THERMAL DIFFUSION FACTORS

The isotopic thermal diffusion factor can be obtained from measurements of the separation that takes place in a precisely constructed column operated under known conditions. According to theory, the separation process in the thermal diffusion column is described for an n-component mixture by the following differential equation:

$$\tau_i = H_o w_i \sum_{j=1}^{n} m_{ij} w_j - K\,(dw_i/dz) + \sigma w_i \quad (1)$$

where

$m_{ij} = (M_i - M_j)/(M_i + M_j)$;

where

M_i and M_j are molecular weights of the components,

τ_i is the net rate of transport of component i along the z direction,

w_i is the mass fraction of component i,

σ is the net mass flow rate through the column section,

H_o is the reduced initial transport coefficient, and

K is the remixing coefficient.

The quantities H_o and K represent complicated integrals involving the geometry and operating conditions of the column and the physical properties of the fluid as functions of temperature. To first order, H_o is proportional to the thermal diffusion factor $\alpha_{T_{ij}}$. The quantity K is independent of $\alpha_{T_{ij}}$.

The steady state separation in the column at total reflux is given by:

$$\ln \frac{(w_i/w_j)_B}{(w_i/w_j)_T} = \ln q_{ij} = H_o m_{ij}\, L/K \quad (2)$$

where

L is the length of the column.

Thus, the average thermal diffusion factor over the temperature range of the column can in principle be obtained from:

$$\alpha_{T_{ij}} = \ln q_{ij}/[\xi L/K] \quad (3)$$

where

ξ is defined as the value of H_o for $\alpha_{T_{ij}}$ equal to unity.

The quantity K is exceedingly sensitive to parasitic circulations caused by nonuniform geometry and temperature distribution; therefore, it is usually better to derive $\alpha_{T_{ij}}$ from experiments that give a result for H_o independent of the parameter K. According to Equation 1 this can be accomplished for conditions such that the transport τ_i is nonzero.

In previous work we have measured steady state separations with a precisely known net flow rate imposed on the column. The development of improved techniques for obtaining very small representative samples has recently allowed us to use transient measurement under total reflux conditions to obtain the equivalent information. Simplex optimization is used to adjust the parameters H_o and K to get the best match between experimental separation results as a function of time and the finite difference solution of the set of partial differential equations describing the time dependent behavior of the column.

In the last report [1] we gave the results of a series of measurements on the C_1 to C_4 normal alkyl chlorides and bromides. These were done mostly at hot to cold wall spacings of 254 and 305 μm. Results for chlorobenzene have been reported earlier [2] for the complete range of spacings from 178 μm to 305 μm.

We have now done additional work with methyl chloride at a spacing of 203 μm and have, in addition, completed one measurement with bromobenzene at 254 μm.

The experimentally measured separations for methyl chloride are plotted in Figure II-1 along with results obtained earlier at a spacing of 254 μm. Parameters derived from the simplex curve fitting procedure are given in Table II-1 as are corresponding values calculated from theory. The initial transport values reported are those for the $CH_3{}^{35}Cl$ - $CH_3{}^{37}Cl$ pair according to the definition:

$$H_{ij} = H_o \, m_{ij}.$$

The theoretical result for H_{ij} at 203 μm is based on $\alpha_{T_{ij}} = 0.0353$ obtained from the previously measured value of H_{ij} at a spacing of 254 μm.

There is reasonably good agreement between theory and experiment for H_{ij} at 203 μm. This, plus the good results obtained for the series with chlorobenzene, suggests that the column is relatively free of parasitics or obstructions to the thermogravitational circulation. The discrepancy between measured and calculated values of K may therefore reflect, in part, the considerable uncertainty in the physical properties of methyl chloride and, in part, the uncertainty in the calculated temperature difference between the hot and cold walls.

The isotopic separation of the $C_6H_5{}^{79}Br$ - $C_6H_5{}^{81}Br$ system was measured as a function of time at a spacing of 254 μm in the 46 cm research column. The results are plotted in Figure II-2, and the parameters derived from fitting the data are given in Table II-2. As in the case of methyl chloride, there is some discrepancy between theoretical and experimental values of the remixing coefficient, K.

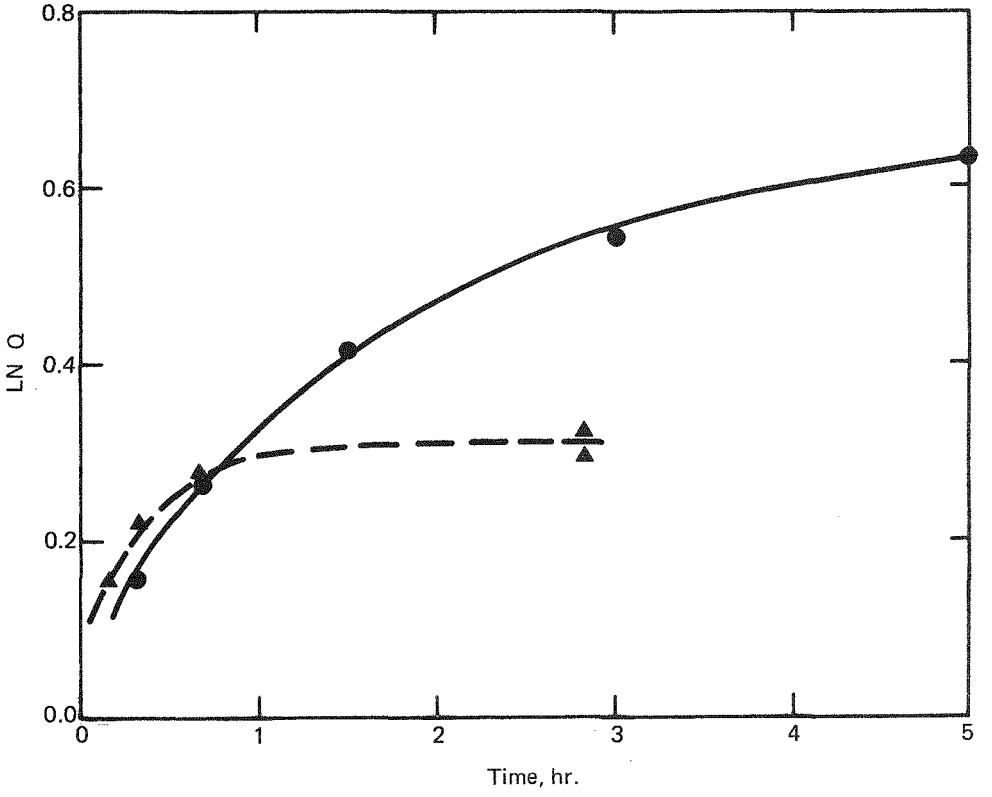

FIGURE II-1 - Separation of the $CH_3{}^{35}Cl$ - $CH_3{}^{37}Cl$ pair in the 45.6 cm research column. The solid circles are for a hot to cold wall spacing of 203 μm, the triangles, for a spacing of 254 μm. The curves are calculated from theory for the best fit.

Table II-1 - COLUMN PARAMETERS AND TRANSPORT COEFFICIENTS FOR LIQUID PHASE THERMAL DIFFUSION EXPERIMENTS WITH METHYL CHLORIDE

	Experiment A	Experiment B
Spacing, μm	254	203
Hot wall temperature, °C	155	153
Cold wall temperature, °C	51	57
Cold wall diameter, cm	1.9286	1.9286
Length, cm	45.56	45.56
$10^5 H_{ij}$ (exptl)	24.9	12.2
$10^5 H_{ij}$ (theory)	---	11.3
K (exptl)	0.036	0.0083
K (theory)	0.026	0.0049
Heat flow (calculated), W	1803	2021
Heat flow (measured), W	1539	1836

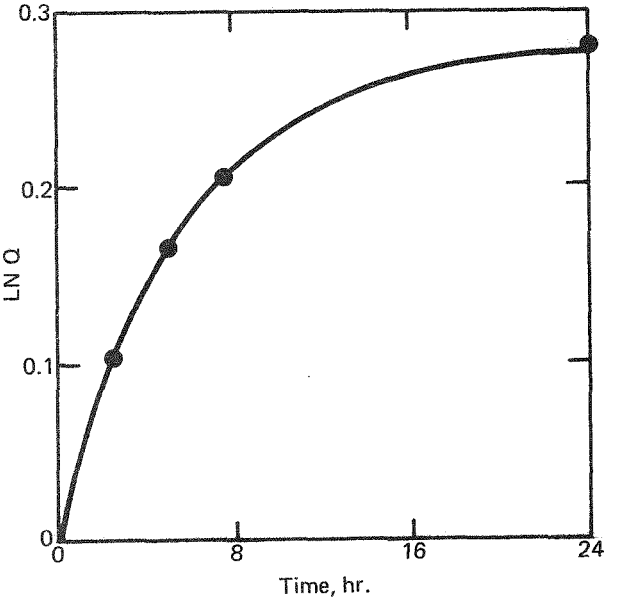

FIGURE II-2 - Separation of the $C_6H_5{}^{79}Br$ - $C_6H_5{}^{81}Br$ pair in the 45.6 cm research column at a spacing of 254 μm. The solid line is the best fit calculated from theory.

Table II-2 - RESULTS OF LIQUID PHASE THERMAL DIFFUSION EXPERIMENTS WITH BROMOBENZENE AT A HOT TO COLD WALL SPACING OF 254 μm

Hot wall temperature, °C	156
Cold wall temperature, °C	46
$10^5 H_{ij}$, g/sec (exptl)	2.89
K, g·cm/sec (exptl)	0.0047
K, g·cm/sec (theory)	0.0037
α_{Tij}	0.0184
α_o	2.89
Heat flow (exptl), W	1402
Heat flow (calculated), W	1606

In the case of bromobenzene, the physical properties are much better known than those of methyl chloride; thus, the difference is most likely the result of error in estimating the effective temperature difference across the working space of the column. A comparison of observed and calculated heat flows supports this hypothesis; however, uncertainties remain in the heat leakage at the ends of the column and in the published values of the thermal conductivity of bromobenzene.

COLUMN PERFORMANCE

It has been apparent for some time that poor performance of liquid phase thermal diffusion columns is nearly always caused by nonideal temperature distribution on the hot and cold walls of the column. Local hot or cold regions result in density changes which in turn give rise to parasitic circulation of fluid and remixing of the column contents. The effects are especially sensitive to column spacing. At spacings equal to or greater than 254 μm, it has been possible to get the performance expected from theory by altering the geometry of the coolant annulus and properly selecting the flowrate of the coolant. These experiments have been described in earlier reports [3].

Recently, we completed a series of experiments aimed at evaluating the extent of the transport of heat in the circumferential direction around the coolant annulus. The experiments were done in a mockup of our current prototype column configuration. The results showed that little transport would take place even at high fluid velocities and Reynolds numbers; therefore, we would not expect local temperature deviations to be suppressed by circumferential flow of heat. It may be possible, however, to achieve a better distribution of temperature by further alteration of the column design.

A new column has now been constructed to test a series of possible column design modifications on the separation of the $C^{32}S^{32}S$ - $C^{32}S^{34}S$ pair at a hot to cold wall spacing of 178 μm. The experiments, which involve evaluations of the separation factor at total reflux, are time consuming because large separations must take place at a relatively slow rate. Seven modifications have now been tested, in addition to three that have not been previously reported for another column of similar construction.

The results given in Table II-3 are encouraging, and a few of the observed separations are significantly higher than those we achieved previously.

The highest separation, q = 114, represents nearly 80% of the total reflux performance expected from theory; however, there is evidence that the transport is somewhat less than that predicted from theory.

BROMINE ISOTOPE SEPARATION

W. M. Rutherford and D. G. Casey

The separation of the isotopes of chlorine in practical quantities at high purities has been described in previous reports [1,4]. Upon completion of the campaign to separate ^{35}Cl, the 14-column experimental liquid thermal diffusion cascade became available for a long-planned campaign to separate the isotopes of bromine.

Table II-3 - RESULTS OF ISOTOPIC SEPARATION MEASUREMENTS WITH CS_2 IN A MODIFIED LIQUID PHASE THERMAL DIFFUSION COLUMN

Steam temperature: 164°C
Water temperature: 15°C
Length: 76.2 cm
Hot wall radius: 0.96065 cm
Cold wall radius: 0.97840 cm

Estimated hot wall temperature: 133°C
Estimated cold wall temperature: 30°C

Column	Modification	Separation Factor	
		Highest Value	End of Experiment
7SC4	1	16.1	8.0
	2	4.6	3.8
	3	15.0	9.8
7SC9	1	12.0	11.4
	2	30	10.2
	3	11.1	---
	4	32	20
	5	69	69
	6	69	49
	7	114	108

Results of work with the 45.6 cm research column suggested that ethyl bromide would have suitable properties as a fluid for the proposed separation; however, preliminary experiments conducted in a 3-column segment of the cascade showed quickly that that compound was unsuitable. A relatively rapid reaction took place between the ethyl bromide and the hot wall of the column, and the corrosion products tended to plug interconnecting capillary lines.

We felt that methyl bromide was a promising alternative, but its considerable toxicity led us to choose bromobenzene for the first campaign.

An experimental separation of bromobenzene was carried out in a 3-column segment to evaluate potential handling and corrosion problems. Results of the test are plotted in Figure II-3 along with results calculated from theory based on a value of 0.0184 for the thermal diffusion factor of the $C_6H_5{}^{79}Br$ - $C_6H_5{}^{81}Br$ pair.

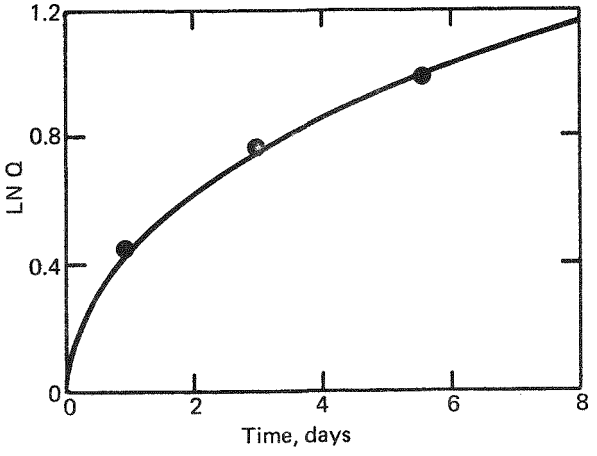

FIGURE II-3 - Isotopic separation of bromobenzene in a 3-column segment of the experimental liquid phase thermal diffusion cascade. The solid line is based on parameters calculated from theory.

There were no apparent difficulties with the 3-column experiment; hence, we began the separation of ^{79}Br in the full length system, which at that time comprised 13 columns. The progress of the separation is plotted in Figure II-4, as are the results of theoretical calculations of the startup process.

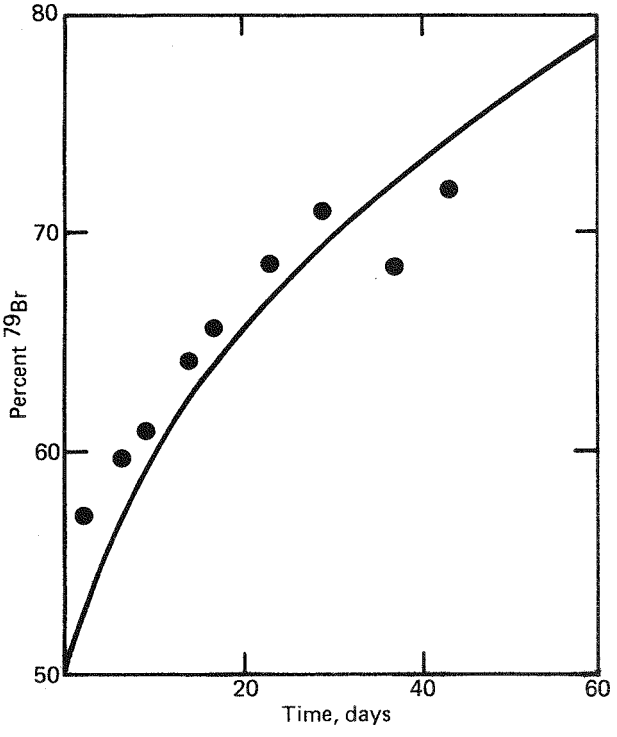

FIGURE II-4 - Separation of ^{79}Br in the experimental 13-column liquid phase thermal diffusion cascade. The disturbance at day 30 is the result of a malfunction in the interstage circulation system.

In the current configuration we predict that some 19 weeks will be required to bring the 18 g product reservoir up to 90% ^{79}Br from the natural abundance concentration of 50.7%. A simple rearrangement of columns, which has not yet been accomplished, is expected to shorten this time considerably.

Calcium isotope separation

W. M. Rutherford

Liquid phase thermal diffusion is being investigated as a means of separating calcium isotopes. A technique has been developed for carrying out the separation with solutions of calcium compounds [5]. Separation of the calcium salt from the solvent is suppressed by setting up a net flow of solvent in a direction counter to the separation of the solute. A 70 cm thermal diffusion column is being used for experimental evaluation of the solvent counterflow concept. A 15 cm column is being used without solvent flow to evaluate compounds and solvents for the process.

EXPERIMENTS WITH SOLVENT FLOW

In a previous report, we presented the results for an experiment which resulted in a significant separation of the calcium isotopes while solvent counterflow was taking place [6]. A separation factor of 1.26 was observed for the ^{40}Ca-^{48}Ca pair in an aqueous solution which initially contained 10 wt % $Ca(NO_3)_2$.

The setup for the experiments, although useful as an interim approach, proved awkward and difficult to control. It made use of continuous feed and withdrawal of solutions at the top of the column to simulate removal and recycle of solvent by distillation.

A solvent distillation apparatus of significantly improved characteristics was designed to replace this arrangement. In addition, new, improved conductivity cells

were fabricated and installed in both top and bottom circulation loops of the column to provide a capability for continuous monitoring of system concentrations. Figure II-5 is a schematic diagram of the revised apparatus.

A systematic evaluation of the $Ca(NO_3)_2 - H_2O$ system is now in progress using the apparatus depicted in Figure II-5. The experiments have as their purpose the determination of the equilibrium separation and the isotopic transport as functions of the solute concentration. In addition, they will serve as tests of how well the solvent counterflow process can be controlled.

Equilibrium runs have now been completed at nominal solute concentrations of 2, 16.7 and 35 wt %. Partial results for the 2 and 16.7% runs are given in Table II-4. Isotopic ratio measurements have not yet been completed on a number of other samples. A 300 ml reservoir was added to the system following the series of measurements at 2%. This accounts for the rather smaller departure from nominal of the solute concentration at the top of the system during the run at 16.7%. The concentration difference across the column was kept at a value constant within ±0.2 wt % by manual control of the solvent injection rate. The concentration at the bottom was made several percent larger than that at the top in order to create a stable density gradient within the column.

The isotopic separations are reported in Table II-4 in terms of the separation factor for the ^{40}Ca-^{48}Ca pair. Thus:

$$q_{48} = (w_{48}/w_{40})_B/(w_{48}/w_{40})_T$$

where w_{48} and w_{40} are the mass fractions of the two isotopes, and the subscripts B and T refer to the bottom and top of the column, respectively. Significant isotopic separations were observed at both nominal concentrations. The slightly higher separations observed for the series of measurements at 2% is not believed at this time to be statistically significant. The separations are, however, much higher than those obtained in the preliminary experiments reported previously [5,6].

EXPERIMENTS WITHOUT SOLVENT FLOW

Exploratory work with the 15 cm column continued. This column is short enough to give a usable range of solute concentrations without solvent counterflow.

Partial results have now been obtained for isotopic separations in 4 systems involving $Ca(NO_3)_2$ as the solute and ordinary and heavy water as solvents. Results are given in Table II-5 in terms of the solute concentrations at the ends of the column and the isotopic separation factor for the ^{40}Ca-^{48}Ca pair.

The isotopic separations are quite large considering the length of the column. There does not appear to be significant difference in isotope effect between D_2O and H_2O as solvents. There is, however, a very significant difference between D_2O and H_2O with respect to solute-solvent separation behavior. The solute-solvent separation factor with D_2O is an order of magnitude smaller than it is for the corresponding H_2O system. This suggests that heavy water systems might be somewhat easier to use for separation of calcium isotopes by liquid phase thermal diffusion.

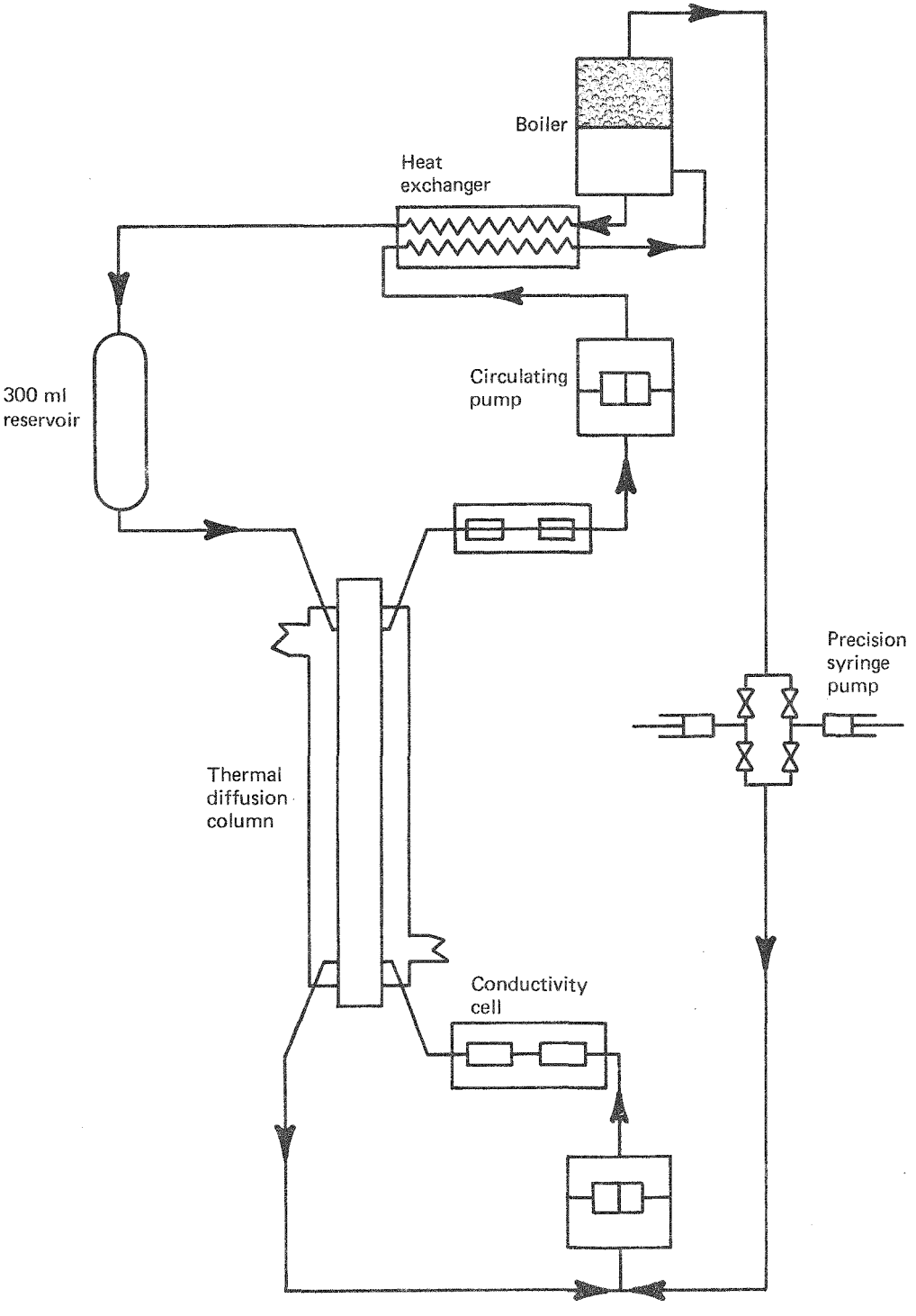

FIGURE II-5 - Solvent recycle apparatus for separation of calcium isotopes by liquid phase thermal diffusion.

Table II-4 - SOLUTE CONCENTRATIONS AND THE SEPARATION OF ^{48}Ca BY LIQUID PHASE THERMAL DIFFUSION WITH SOLVENT COUNTERFLOW

Time (days)	Solvent Injection Rate (ml/hr)	Solute Concentration (wt %) Top	Solute Concentration (wt %) Bottom	ln q_{48}
A. Nominal 2% $Ca(NO_3)_2$, Experiment 1				
4	0.754	1.31	4.47	0.272
7	0.804	1.18	4.40	0.360
11	0.854	1.25	3.96	0.387
B. Nominal 2% $Ca(NO_3)_2$, Experiment 2				
14	0.854	1.25	3.83	0.303
20	0.854	1.12	3.25	0.368
C. Nominal 16.7% $Ca(NO_3)_2$				
26	0.439	16.84	20.73	0.307
29	0.439	16.84	20.73	0.294

Table II-5 - SEPARATION OF CALCIUM ISOTOPES WITHOUT COUNTERFLOW IN A 15 cm LIQUID PHASE THERMAL DIFFUSION COLUMN

Time (days)	Solute Concentration (wt %) Top	Solute Concentration (wt %) Bottom	ln q_{48}
A. $Ca(NO_3)_2$ in H_2O[a]			
7	0.066	20.90	0.257
6	0.076	25.34	0.212
18	0.036	29.89	0.271
B. $Ca(NO_3)_2$ in D_2O			
7	0.577	19.14	0.214
10	0.577	19.20	0.213
17	0.577	19.20	0.131
C. $Ca(NO_3)_2$ in D_2O			
12	1.21	39.00	0.227
17	1.21	38.96	0.103

[a]Each sampling required that a large volume be removed from the top in order to provide sufficient solute for analysis. This resulted in a substantial shift in the average concentration as the experiment continued.

Calcium chemical exchange

B. E. Jepson

Heavy calcium isotopes were slightly enriched by chemical exchange chromatography using columns packed with resin-bound 222B cryptand. An ethanol solution of calcium chloride was used as the fluid phase. Six isotopic analyses of samples selected from samples numbered 638 (breakthrough) to sample number 672 showed enrichments. No clear isotopic enrichment gradient was evident, however, as a result of scatter in the data; and more samples in this range are being analyzed. Calcium-48 concentrations in this sample region ranged from 0.20% to 0.23% compared to 0.186% for the feed material. Calcium-44 concentrations ranged from 2.15% to 2.20% compared to 2.08% for the feed solution. The total amount of calcium collected in the above sample range was approximately 40 mg.

Mutual diffusion

W. L. Taylor and D. Cain

In our last report in this series [7] we presented our revised data for the argon-helium system. A major factor in the revision was the application of corrections to the mass spectrometer results which account for different pumping speeds of the two gases present in the binary mixtures that were analyzed [8,9]. In this report we present diffusion coefficients for argon-neon (see Table II-6) which were analyzed using the procedure given in Reference 7. The corrections to the mass spectrometer analyses due to the difference in pumping speeds between argon and neon were much smaller than for argon/helium mixtures, as one would expect. A further possiblity of error was considered in the argon/neon analysis. This can be due to the inability to resolve the singly ionized ^{20}Ne peak from doubly ionized ^{40}Ar. Because the ionization potential on the instrument is set at a rather high level for the analyses, a significant fraction of $^{40}Ar^{++}$ is produced, and a correction must

Table II-6 - DIFFUSION COEFFICIENTS OF ARGON-NEON AT ONE ATMOSPHERE PRESSURE, EQUILIBRIUM CONCENTRATION

Temperature (K)	D_{12} (cm^2/sec)
350	0.424
357	0.454
441	0.625[a]
497	0.804
511	0.845
541	0.907[a]
622	1.179
642	1.260
647	1.311[a]
700	1.424
768	1.639[a]
782	1.757
798	1.856
891	2.138
907	2.222[a]
933	2.311
953	2.441
1022	2.686[a]
1097	3.089
1100	3.075[a]
1193	3.488
1201	3.605[a]
1293	4.062

[a]Experiments were performed using isotopically pure ^{22}Ne as feed gas. A small correction was applied to convert the values to the atomic weight of naturally occurring isotopic abundance neon.

be applied to resolve the peak height. In order to test the validity of this procedure, eight experiments were performed throughout the temperature range using ^{22}Ne with argon as the feed gases. The ^{22}Ne was better than 99.9% pure with no significant mass-20 peak observable. In order to directly compare the $^{22}Ne/Ar$ diffusion coefficients with those obtained using natural abundance neon, the following mass correction was applied:

$$\left[\frac{2\,M_{nat.abd.}}{M_{nat.abd.} + M_{40}}\right]^{1/2} \Big/ \left[\frac{2\,M_{22}}{M_{22} + M_{40}}\right]^{1/2}$$

$$= 0.97221$$

$$\left[D_{12}\right]_{nat.abd.} = \left[D_{12}\right]_{22} / 0.97221$$

The results are also given in Table II-6 and the composite data are shown as deviations from the Marrero and Mason [10] correlation in Figure II-6. It is seen from the figure that, after the mass correction is made, no difference can be distinguished (within the experimental scatter) between the experiments using ^{22}Ne or natural abundance neon as feed gas. It is also seen that the present results agree with the Russian work [11] but are higher than the data of Hogervorst [12], as we have observed previously in other mixtures. The dot-dashed line (·—·) is the diffusion coefficient calculated from experimental viscosities through the mutual consistency relations [13,14] and lies about midway between the present experimental data and those of Hogervorst.

In a previous report [8] we showed that the best currently available thermal diffusion factors for neon-argon are not consistent with either the Marrero and

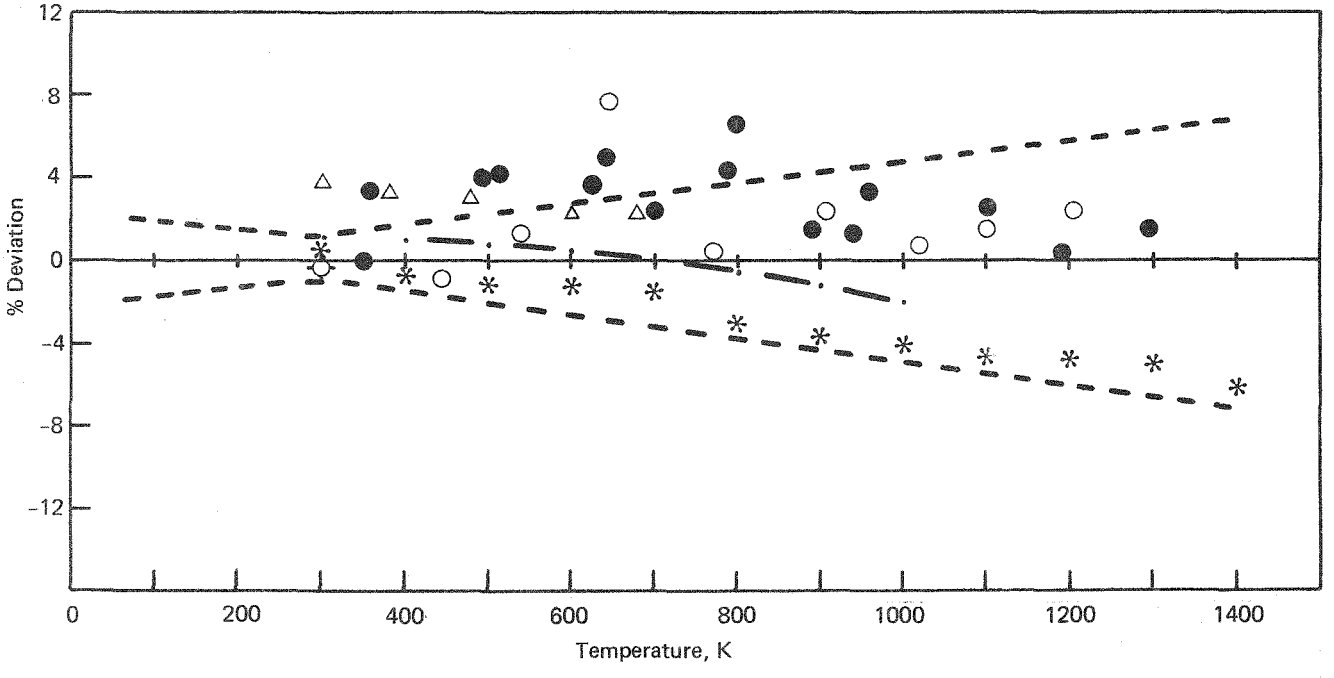

FIGURE II-6 - Percent deviation of experimental diffusion coefficients from the Marrero and Mason correlation function. The experimental points are those measured subsequently to and not included in the correlations. They are: ●, present data using natural isotopic abundance neon; ○, present data using pure ^{22}Ne; *, Hogervorst (Ref. 5); △, Kalinen and Suetin (Ref. 6); and ☼, Arora, et al. (Ref. 7). The curves are: Abscissa (or base line), Marrero and Mason correlation function with ±---, the reported uncertainty in the correlation (Ref. 4); and —·—, D_{12} values derived from viscosity data (Ref. 8,9).

Mason (M&M) correlation or Hogervorst's data. We have developed the following procedure for determining the parameters in a M&M-type function from thermal diffusion data, and have found the resulting functions to agree with the original correlating function to better than 1%.

According to the mutual consistency relations, $\alpha_T = (6C_{12}^* - 5)X_T$, where X_T is a complicated expression which contains the masses, mole fractions, diffusion coefficients, viscosities, temperatures, and collision integrals for the components of interest. At a fixed temperature and a given pair of gases, X_T is a constant. The factor $(6C_{12}^* - 5)$ is expressed in the following form:

$$(6C_{12}^* - 5) = 2[2 - (\partial \ell nD_{12}/\partial \ell nT)_p] \quad (1)$$

If a M&M-type correlating function is assumed, then the derivative which appears above becomes:

$$(\partial \ell nD_{12}/\partial \ell nT)_p = s + \frac{2}{\ell n(\phi_o/k)} + \frac{S}{T} + \frac{2S'}{T^2} \quad (2)$$

Another expression for the logarithmic derivative can be obtained by inverting Equation 1:

$$(\partial \ell nD_{12}/\partial \ell nT)_p = 2 - (6C_{12}^* - 5)/2 = 2 - \alpha_T/2X_T \quad (3)$$

Combining Equations 2 and 3 and transposing the ϕ_o/k term yields an expression amenable to a least squares fitting procedure:

$$2 - \alpha_T/2X_T - \frac{2}{\ell n(\phi_o/kT)} = s + S/T + 2S'/T^2 \quad (4)$$

The values of ϕ_o/k appearing in Equation 4 are taken from independent SCF-HF calculations, where available, and from molecular beam experiments otherwise. With these values of ϕ_o/k, experimental α_T values, and X_T terms as taken from the mutual consistency relations, the LHS of Equation 4 is submitted to a least-squares procedure in order to determine the parameters s, S, and S'.

Having determined the values of ϕ_o/k, s, S, and S', the only undetermined parameter in a M&M correlating function is the constant term A. This situation can be resolved by forcing the correlating function through an experimental data point. The accurate data of Arora, et al. [15] at 300 K have been used.

The results of this procedure are summarized in Table II-7.

Table II-7 - PARAMETERS FOR THE M&M CORRELATION FUNCTION FOR DIFFUSION AS DERIVED FROM THERMAL DIFFUSION DATA

System	$\ell n(\ _o/k)$	ϕ_o/k	Source	S	S	S'	A
He-Ar	17.1933	2.9306×10^7	SCF-HF	1.5213	4.47096	---	0.01718
Ne-Ar	18.07448	7.0737×10^7	SCF-HF	1.47398	24.86	677.573	0.01215
Xe-Ar	22.02618	3.68×10^8	beam	1.46281	99.9198	---	0.01009

Molecular beam scattering

R. W. York

The neon dimer experiments have been completed. We found during the data reduction that the dimer concentration was not nearly as high as predicted. Analysis of the experimental technique suggested that the beam dimer particles were being fragmented by the election energy in the ionizer portion of the quadrupole detector. This would then prevent their detection as dimers by the quadrupole/multiplier. One final attempt will be made to observe the neon dimers without dissociating them into single atoms. A single threshold experiment will be run at low source temperature using the minimum electron energy required to ionize the neon atoms. If this energy is dissociative, the indication will be that dimers cannot be detected by our present beam detector system even though they exist in the beam.

The new, triple-pumped detector system was found to be internally contaminated upon receipt from the fabricating vendor. The contaminant, a polyethylene-type substance, had coated all of the internal surfaces. After much analysis and experimentation, we found that it could be effectively removed with a sulphuric acid/no chrome-mix solution at a temperature of about 85°C, and the resulting stainless steel surface etched for vacuum preparation with a dilute hydrochloric acid bath. The technique and hardware to implement this process were developed at Mound, and the system was returned to the vendor for cleaning under the supervision of a Mound technician.

The cleaning process has been successfully completed, and the detector system has been returned to Mound. Final assembly and leak testing are now under way. This leak test is performed under final use conditions using ion pumps and copper vacuum seals on all ports. During these tests, a determination will be made on the ultimate vacuum capability of the system prior to installation in the molecular beam chamber with the quadrupole detector system housed inside.

III. Metal hydride studies

NMR studies of hydrogen diffusion in $TiCr_2H_x$

R. C. Bowman, Jr., B. D. Craft and A. Attalla

The Laves structure intermetallic $TiCr_2$ can form either a cubic (C15) or hexagonal (C14) phase. Both of these phases react [1,2] with hydrogen to form $TiCr_2H_x$ phases. These hydrides provide the opportunity to study the roles of structure modification while retaining the same number and kind of metal atoms. The proton relaxation times have been measured for both low and intermediate hydrogen concentrations in the C14 and C15 forms of $TiCr_2$. The proton relaxation time data for $TiCr_{1.8}H_{0.55}$ and $TiCr_{1.8}H_{2.5}$ are summarized in Figures III-1 and III-2, respectively. Both hydrides have cubic C15 crystal structure. Similar NMR data have also been recently obtained for $TiCr_2H_{0.93}$ and $TiCr_{1.9}H_{2.9}$ which have the hexagonal C14 structure. The relaxation times for all these phases indicate very rapid diffusion rates (i.e., $\sim 10^{-8}$ $cm^2/sec \leq D \leq 10^{-6}$ cm^2/sec at 300K), and their activation energy (E_a) values over various temperature regions are given in Table III-1. The diffusion behavior in

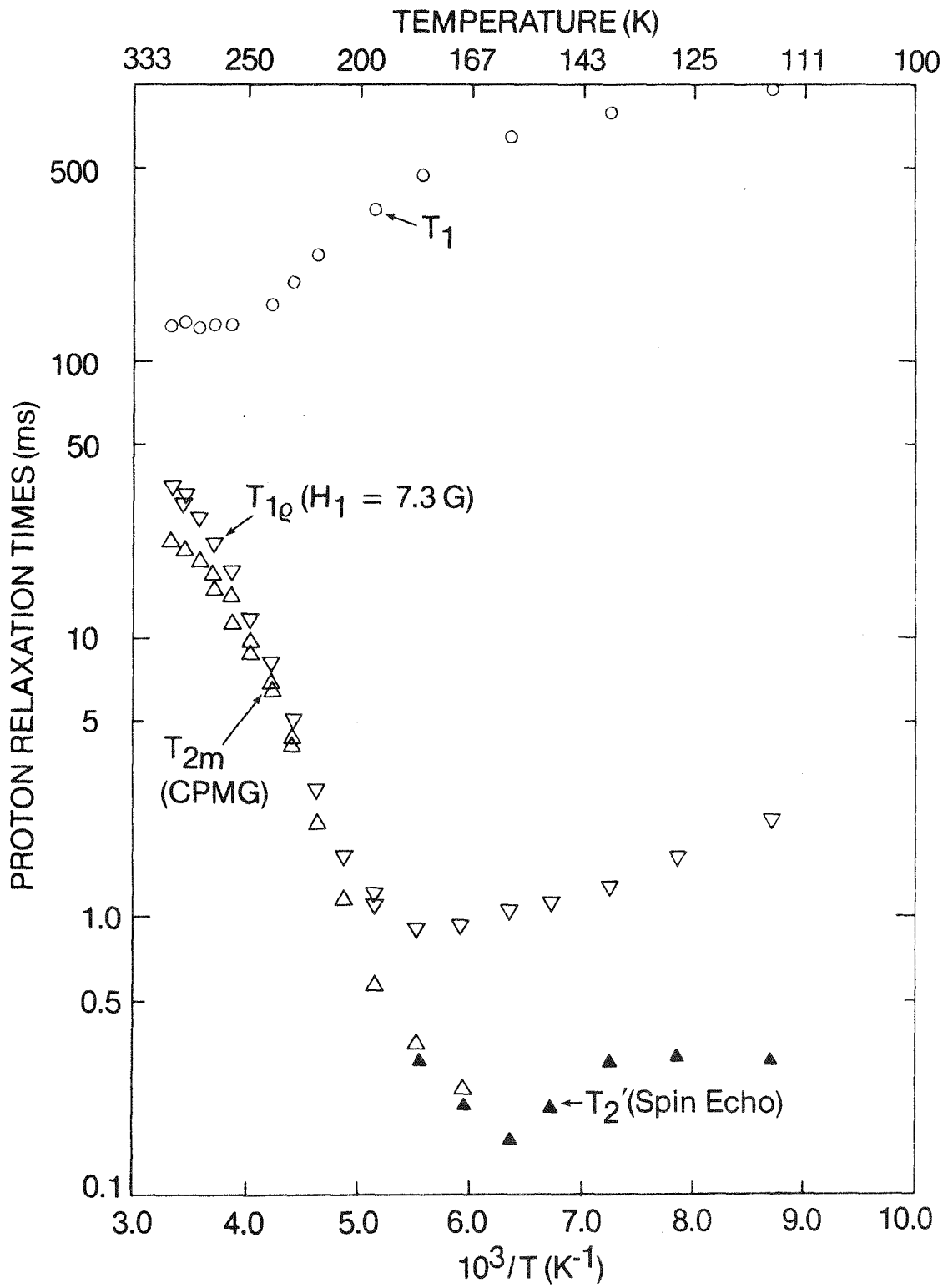

FIGURE III-1 - Proton relaxation times for cubic α-$TiCr_{1.8}H_{0.55}$ measured at 34.5 MHz.

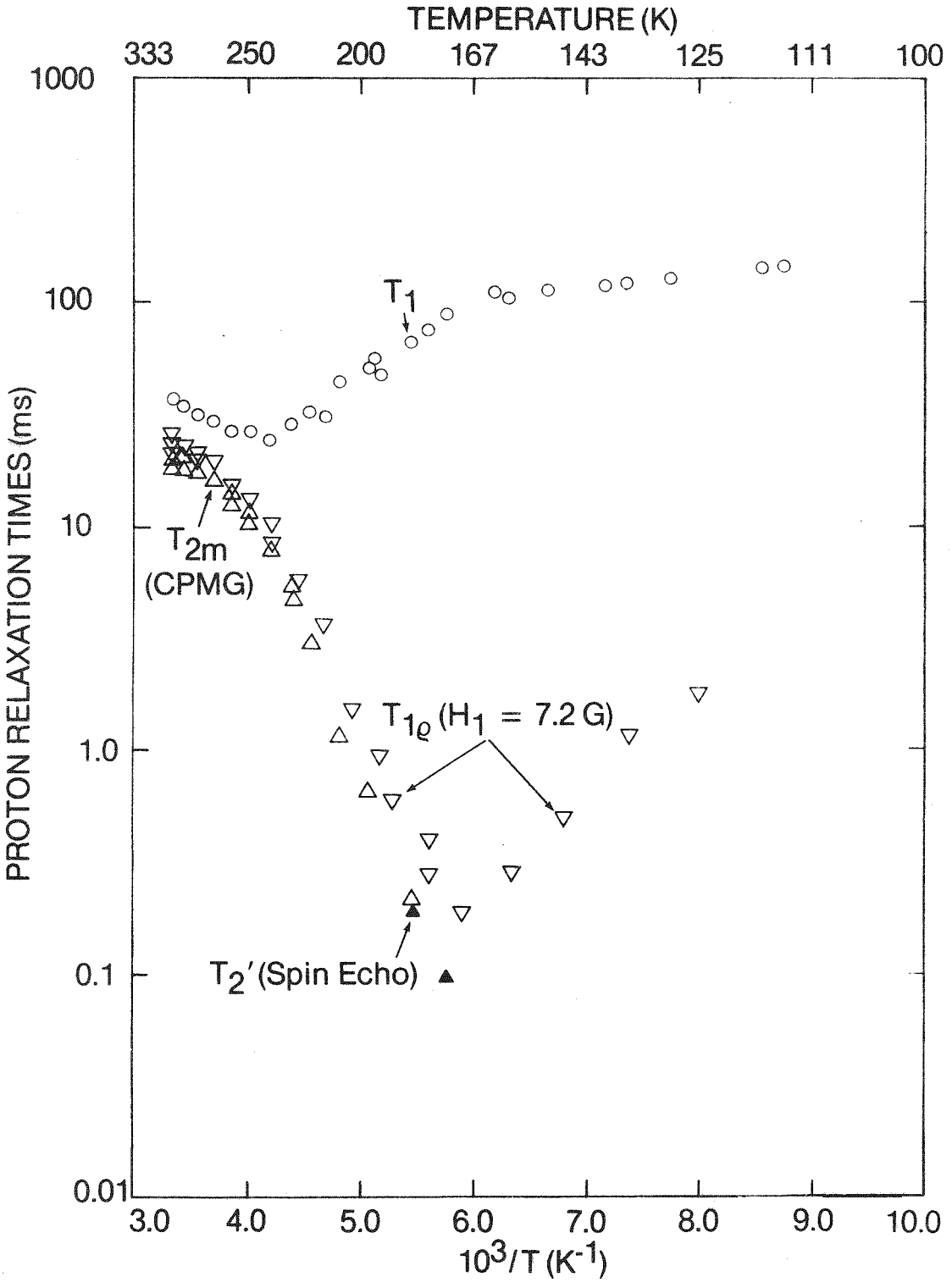

FIGURE III-2 - Proton relaxation times for β-$TiCr_{1.8}H_{2.5}$ measured at 34.5 MHz.

Table III-1 - SUMMARY OF DIFFUSION ACTIVATION ENERGIES FOR $TiCr_2H_x$ OBTAINED FROM PROTON NMR STUDIES

Composition	Structure of Laves Phase	Temperature Range (K)	E_a (eV)
$TiCr_{1.8}H_{0.55}$	C15	190 - 280	0.195 ± 0.02
		115 - 170	0.03 ± 0.01
$TiCr_{1.8}H_{2.5}$	C15	180 - 280	0.255 ± 0.02
		120 - 170	0.10 ± 0.01
$TiCr_{1.9}H_{0.93}$	C14	190 - 290	0.215 ± 0.01
		105 - 160[a]	0.045 ± 0.01
$TiCr_{1.9}H_{2.9}$	C14	210 - 280	0.39 ± 0.02
		120 - 175[a]	0.19 ± 0.02
$ZrMn_2H_x$[b]	C14	170 - 220	0.16 ± 0.03
$HfV_2H_{2.1}$[b]	C15	200 - 270	0.19 ± 0.01

[a] Nonexponential $T_{1\rho}$ and T_2 relaxation behavior in this temperature range.

[b] J. Shinar, et al., Zeit, Physk. Chem. N.F., 117, 69 (1979).

the various $TiCr_2H_x$ samples is rather complex and difficult to interpret without more detailed crystal structure determinations. All the $TiCr_2H_x$ samples, however, except cubic $TiCr_{1.8}H_{0.55}$, exhibit the typical proton relaxation time behavior below 150 K where hydrogen motion decreases with cooling to ultimately reach the immobile rigid lattice limit. The nonexponential $T_{1\rho}$ and T_2 recoveries (but with exponential T_1) for the C14 $TiCr_{1.9}H_x$ samples probably reflect H-atoms occupying inequivalent sites with differing diffusion characteristics.

The T_2 spin-echo data below 150 K in Figure III-1 are ten times longer than several reasonable estimates for immobile proton in cubic (C15) $TiCr_{1.8}H_{0.55}$. These results imply a nearly temperature independent motion that can reduce the rigid lattice proton interactions by an order of magnitude. Recent unpublished neutron diffraction studies of $TiCr_{1.8}D_x$ from the Brookhaven group indicate the D-atoms occupy only the tetrahedral Ti_2Cr_2 sites of the C15 structure. When $x \leq 2$, a single H-atom is randomly occupying a set of six equivalent sites. The low temperature proton relaxation times for $TiCr_{1.8}H_{0.55}$ may reflect residual motion around these sites for each singly occupied hexagon - possibly through a "tunneling" mechanism. This process should yield the greatly reduced and nearly constant T_2 relaxation below 150 K. The E_a values of 0.2 eV for the $TiCr_{1.8}H_x$ samples above 180 K would correspond to a long-range motion where H-atoms jump from an occupied hexagon to a neighboring empty hexagon. When $x > 2$ (as for $TiCr_{1.8}H_{2.5}$), there would be more than one H-atom on some hexagons. Consequently, short-range repulsive correlations would probably prevent local ring motion to yield the observed normal rigid lattice behavior at low temperatures. Furthermore, when the crystal symmetry is lowered from C15 to C14, all the Ti_2Cr_2 sites are no

longer equivalent and tunneling among the sites would again not be expected. This qualitatively accounts for the difference between C15 $TiCr_{1.8}H_{0.55}$ and C14 $TiCr_{1.9}H_{0.93}$. However, more structural information on the low temperature site occupancies of H-atoms in the C14 and C15 $TiCr_2H_x$ phases are required before the diffusion processes can be firmly identified.

A comprehensive evaluation of the proton relaxation times for these four $TiCr_2H_x$ samples is currently in progress to provide a more quantitative assessment of hydrogen diffusion behavior in both the C14 and C15 structures. In order to obtain a better understanding of the unusual low temperature diffusion behavior in α-phase cubic (C15) $TiCr_{1.8}H_x$, additional NMR experiments are being conducted on several samples with compositions in the range $0.39 \leq x \leq 1.01$.

References

I. Low temperature research

1. Mound Facility Activities in Chemical and Physical Research: January-June 1980, MLM-2756 (August 29, 1980), pp. 15-16.

2. J. W. Pyper, et al., UCRL-52391, Lawrence Livermore Laboratory, January 1978.

3. G. K. Boreskov, in Fundamentals of Gas-Surface Interactions, H. Saltsburg, J. N. Smith and M. Rogers, Eds., Academic Press, 1967, pp. 216-242.

4. S. C. Lind, Radiation Chemistry of Gases, Reinhold, New York, 1961, Chapter 10.

5. Stable Gaseous Isotope Separation and Purification: April-June 1967, MLM-1419 (October 31, 1967), p. 17.

6. Mound Facility Activities in Chemical and Physical Research: July-December 1980, MLM-2809 (April 10, 1980), p. 16.

7. Mound Facility Activities in Chemical and Physical Research: July-December 1979, MLM-2727 (June 18, 1980), p. 17.

8. Stable Gaseous Isotope Separation and Purification: July-September 1966, MLM-1367, p. 26.

9. Stable Gaseous Isotope Separation and Purification: October-December 1967, MLM-1455, p. 23.

II. Separation research

1. Mound Facility Activities in Chemical and Physical Research: July-December 1980, MLM-2809 (April 10, 1981), p. 19.

2. Mound Facility Activities in Chemical and Physical Research: July-December 1979, MLM-2727 (June 18, 1980), p. 21.

3. Mound Facility Activities in Chemical and Physical Research: January-June 1979, MLM-2654 (October 29, 1979), p. 12.

4. Mound Facility Activities in Chemical and Physical Research: January-June 1980, MLM-2756 (August 29, 1980), p. 17.

5. W. M. Rutherford and K. W. Laughlin, Science, 211, 1054 (1981).

6. Mound Facility Activities in Chemical and Physical Research: July-December 1980, MLM-2809 (April 10, 1981), p. 21.

7. Mound Facility Activities in Chemical and Physical Research: July-December 1980, MLM-2809 (April 10, 1981), p. 28.

8. R. E. Ellefson, "Factors Involved in Quantitative Gas Analysis by Mass Spectrometry," presented at the 22nd Rocky Mountain Conference, Rocky Mountain Society for Applied Spectroscopy and R. M. Chromatography Group, Denver, Colorado, August 11-14, 1980, MLM-2794(OP).

9. R. E. Ellefson, "Systematic Error in Isotopic Analysis of Noble Gas Mixtures," presented at the 29th Annual Conference on Mass Spectrometry and Allied Topics, May 25-29, 1981, Minneapolis, Minnesota.

10. T. R. Marrero and E. A. Mason, J. Phys. Chem. Ref. Data, 1, 1 (1972).

11. B. A. Kalinen and P. E. Suetin, Heat Transfer - Sov. Res., 7, 146 (1975).

12. W. Hogervorst, Physica, 51, 59 (1971).

13. Mound Facility Activities in Chemical and Physical Research: January-June 1980, MLM-2756 (August 29, 1980), p. 45.

14. J. Kestin, W. Wakeham and K. Watanabe, J. Chem. Phys., 53, 3773 (1970).

15. P. S. Arora, H. L. Robjohns and P. J. Dunlop, Physica, 95A, 561 (1979).

III. Metal hydride studies

1. J. R. Johnson and J. J. Reilly, Inorg. Chem., 17, 3103 (1978).

2. J. R. Johnson, J. Less-Common Metals, 73, 345 (1980).

Distribution

EXTERNAL

TID-4500, UC-4 and UC-22 (194)
H. N Hill, DOE/Dayton Area Office
E. L. Venturini, Sandia National Laboratories, Albuquerque
R. K. Flitcraft, Monsanto Research Corporation
W. J. Haubach, DOE/Office of Basic Energy Sciences
F. D. Stevenson, DOE/Office of Basic Energy Sciences
J. Burnett, DOE/Office of Basic Energy Sciences
N. Haberman, DOE/Division of Nuclear Energy
J. R. Blair, DOE/Office of Health and Environmental Research
J. N. Maddox, DOE/Office of Health and Environmental Research
D. White, University of Pennsylvania
Monsanto Reports Library, R2C, St. Louis

INTERNAL

W. R. Amos
L. R. Baird
R. C. Bowman
D. Cain
W. T. Cave
C. W. Huntington
B. E. Jepson
G. T. McConville
E. D. Michaels
G. C. Shockey
G. L. Silver
W. M. Rutherford
W. L. Taylor
R. E. Vallee
W. R. Wilkes
L. J. Wittenberg
R. W. York
Document Control
Library (15)
Publications

Published by Information Services
Stephen L. Nowka, Editor